Electrowetting at a liquid metal-semiconductor junction

S. Arscott, Matthieu Gaudet

Electrowetting at a liquid metal-semiconductor junction

Cite as: Appl. Phys. Lett. **103**, 074104 (2013); https://doi.org/10.1063/1.4818715
Submitted: 13 March 2013 • Accepted: 28 July 2013 • Published Online: 15 August 2013

Steve Arscott and Matthieu Gaudet

Electrowetting at a liquid metal-semiconductor junction

Steve Arscott[a] and Matthieu Gaudet
Institut d'Electronique, de Microélectronique et de Nanotechnologie (IEMN), CNRS UMR8520, The University of Lille, Cité Scientifique, Avenue Poincaré, 59652 Villeneuve d'Ascq, France

(Received 13 March 2013; accepted 28 July 2013; published online 15 August 2013)

We report electrowetting at a liquid metal-semiconductor (Schottky) junction using of a mercury droplet resting on silicon. This is demonstrated using n-type and p-type single-crystal silicon wafers of different doping levels. The voltage-dependent wetting contact angle variation of the mercury droplet is observed to depend on both the underlying semiconductor doping density and type. The electrowetting behavior can be explained by the voltage-dependent modulation of the capacitance of a Schottky junction; current-voltage and capacitance-voltage measurements indicate this to be the case. A modified Young-Lippmann electrowetting equation—formulated using a well-established metal-semiconductor junction model—agrees well with the observations. © *2013 AIP Publishing LLC*. [http://dx.doi.org/10.1063/1.4818715]

Two well-known physical effects are rectification[1] discovered by Ferdinand Braun in 1874 and electrowetting[2] stemming from the work of Gabriel Lippmann in 1875. The metal-semiconductor contact[3] is one of the workhorses of the microelectronics revolution[4] whilst modern electrowetting-on-dielectric (EWOD)[5]—using a liquid-insulator-conductor junction—has many applications[6–14] including displays,[6] droplet transport,[7,8] smart optics,[9,10] electronic paper,[11,12] miniaturized chemistry,[13] and energy harvesting.[14] Here, electrowetting is reported at a rectifying liquid metal-semiconductor (Schottky) junction[15,16]—effectively combining the two effects.

Electrowetting[5] can be understood using the following equation:

$$\cos\theta(V) = \cos\theta_0 + \frac{E(V)}{\gamma}, \tag{1}$$

where $\theta(V)$ is the voltage V dependent contact angle of a droplet resting on a surface, θ_0 is the contact angle of the droplet at zero bias, and γ is the surface tension of the liquid. In the case of EWOD, the energy term $E(V)$ (per unit surface) corresponds to the stored electrical energy in the capacitive layer, i.e., $\frac{1}{2}CV^2 - C$ (per unit surface) does not vary with voltage. By replacing the conductor by a semiconductor, an optically induced wetting transition and a voltage-polarity dependent wetting transition have recently been demonstrated using an electrolyte-insulator-semiconductor system[17]—it follows thus that original wetting transitions may also be associated with the dissymmetrical electrical nature of a liquid metal-semiconductor junction.[18–21]

Fig. 1 illustrates electrowetting of a perfectly conducting droplet which forms a Schottky junction at the surface of a semiconductor. At thermal equilibrium the Fermi level (short dashed line) in the semiconductor lines up with the top of the conduction band in the conducting droplet (shaded region)—the droplet will form a zero-bias contact angle θ_0 with the surface of the semiconductor. Under reverse bias, the capacitance of the junction decreases causing the contact angle of the conducting droplet—indicated by the long dashed line—to decrease as the reverse bias is increased. In order to demonstrate the effect a liquid metal-semiconductor contact, such as Hg-Si,[22–28] can be used. Indeed, mercury has successfully been used to demonstrate and apply EWOD.[8,29]

Fig. 2 shows photographic evidence of electrowetting at a Schottky junction (see also Ref. 30). Small droplets of mercury—having a diameter less than the capillary length ~1.9 mm - were placed directly onto the prepared silicon wafers.[30] Removal of the oxide prior to Hg deposition produces a Schottky contact.[23,24,26,28] Fig. 3 shows the variation of contact angle—extracted using software[31]—with applied voltage (open circles data) for n-type and p-type silicon. An electrowetting effect was observed for all wafers tested. The contact angle reduces upon increasing reverse bias—by ~2.5° for n-type (0 to −20 V) and ~5° for p-type (0 to 30 V) - the electrowetting occurs only under reverse bias. The role of the semiconductor doping density is also apparent: the higher doped p-type wafer has a larger contact angle variation. The droplet contact radius is seen to increase when increasing the reverse bias voltage—the value of droplet contact radius

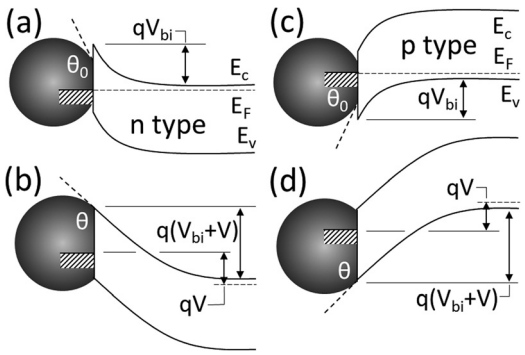

FIG. 1. Energy band diagrams of electrowetting of a conducting droplet (grey) at a Schottky junction under different bias conditions. (a) n-type at thermal equilibrium. (b) n-type under reverse bias—a negative voltage applied to the droplet. (c) p-type at thermal equilibrium and (d) p-type under reverse bias—a positive voltage applied to the droplet. E_c, bottom of the conduction band; E_F, Fermi level; E_v, top of the valence band and V_{bi} = built-in voltage of the junction.

[a]Electronic mail: steve.arscott@iemn.univ-lille1.fr

variation is greater for the higher doped p-type wafer. The droplet contact surface is observed to increase significantly upon application of reverse bias voltage: ~10% for the n-type wafer (at −20 V) and ~15% for the p-type wafer (at 40 V); this observation could have implications for mercury based contact measurements in semiconductor studies, see later. The electrowetting is reversible—turning off the reverse bias enables the zero-bias contact angles to be restored. Contact angle saturation[32,33] is also apparent from the data—for the n-type silicon, saturation begins at −20 V whereas for the p-type silicon it begins at 30 V. Contact angle saturation for EWOD is a well-documented phenomenon[32] which still defies a total understanding.[33] The measured contact angle variation indicates the importance of the role of the Schottky junction and hence the importance of parameters such as doping density, barrier height, built-in voltage, and surface states. In order to characterize the Schottky diodes, we have conducted electrical measurements.

Fig. 4 shows current-voltage (*I–V*) measurements performed on the Hg-Si Schottky junctions used for the electrowetting experiments. The purpose of the *I–V* measurements was twofold: (i) to be sure that the Hg-Si systems—used for the electrowetting experiments—behave as Schottky diodes in reverse bias[22–28] (ii) to measure the barrier heights and built-in voltages of the Hg-nSi and Hg-pSi used for the electrowetting systems (see Ref. 30 for parameter extraction method).

The *I–V* measurements indicate that the Hg-Si contacts are functioning as reverse bias Schottky diodes. The zero-bias junction surfaces were measured to be $1 \times 10^{-6}\,m^2$ (n-type) and $6.7 \times 10^{-7}\,m^2$ (p-type). The measured current densities *J*—plotted in Fig. 4—are consistent with previous studies using silicon wafers having similar restivities.[22–28] For the Hg-nSi contact, $J = 2.3 \times 10^{-5}$ A m^{-2} at −1 V rising to 11 A m^{-2} at −15 V and 50 A m^{-2} at −20 V [Fig. 4(a)]—comparable to the litterature[22,25,26] following surface treatment with HF. For the Hg-pSi contact, we observe $J = 2 \times 10^{-3}$ A m^{-2} at 1 V rising to 3.7 at 15 V and 22.4 A m^{-2} at 25 V [Fig. 4(b)]—comparable to the litterature[22–24] following surface treatment with HF. The apparent reverse bias breakdown voltages are comparable with those given in Ref. 23. The barrier heights ϕ_b of the Hg-nSi and Hg-pSi junctions were measured to be 0.82 eV and 0.77 eV—thus V_{bi} can be calculated to be 1.1 V and 1.01 V for the n-type and the p-type Hg-Si junctions using the precise doping densities obtained using the capacitance-voltage (*C–V*) measurements.

The *I–V* measurements also suggest an explanation for the observed contact angle saturation—Fig. 3 (open circle data). The higher reverse bias leakage currents at voltages above −20 V for the n-type and 25 V for the p-type suggest that the junction can no longer be considered to be a near perfect capacitor; in this case, Eq. (1) no longer holds—due to energy loss—and one would not expect the contact angle to decrease when increasing the reverse bias voltage further. At higher reverse bias, current spikes are sometimes observed during the *I–V* measurements [Fig. 4(b)] and during the electrowetting experiments, however, the contact angle is not observed to change abruptly when this is the case.

Small signal *C–V* measurements, shown in Fig. 5, were performed using the silicon wafers used for the electrowetting experiments for several reasons: (i) to measure the precise doping density level of the silicon wafers, (ii) to measure the *areal* capacitance as a function of applied voltage and frequency, (iii) to estimate the surface state density at the silicon surfaces, and (iv) to measure the series resistance introduced by the Si wafer. Depending on pre-treatment of the silicon surface,[3] aluminum is known to form good Schottky contacts to both n and p-type silicons.[34] Use of a solid metal contact allows the extraction of *C* as the surface area is constant. Indeed, the surface treatment prior to

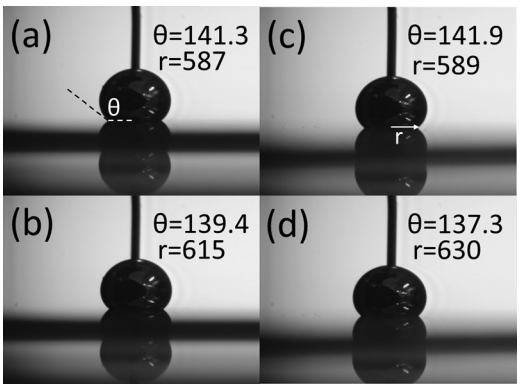

FIG. 2. Evidence of electrowetting at the mercury-silicon Schottky junction. (a) n-type silicon at zero bias. (b) n-type silicon at a reverse bias of −20 V. (c) p-type silicon at zero bias and (d) p-type silicon at a reverse bias of +40 V. The measured contact angles θ (deg) and radii *r* (μm) of droplet contact surface are given.

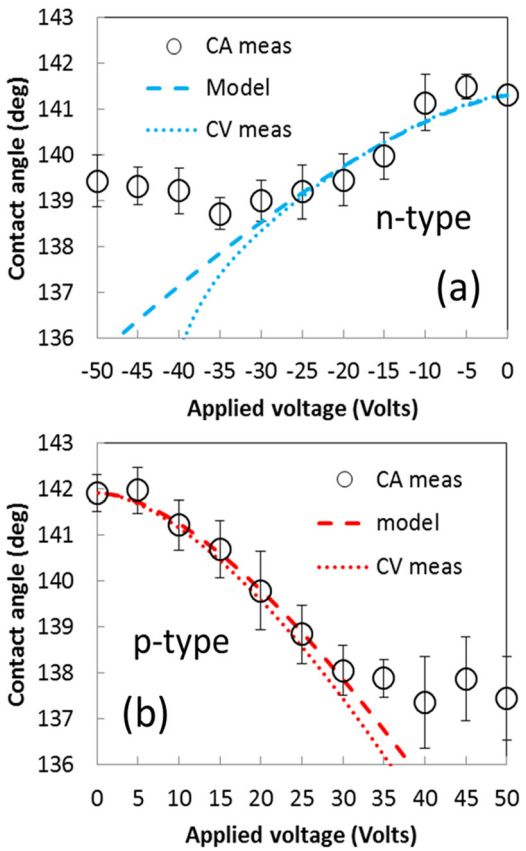

FIG. 3. Contact angle versus voltage for the mercury-silicon Schottky junctions. (a) n-type silicon and (b) p-type silicon (open circles). Thick solid lines indicate the modeled curves based our model, Eq. (2). Thin dashed lines obtained from the *C–V* measurements.

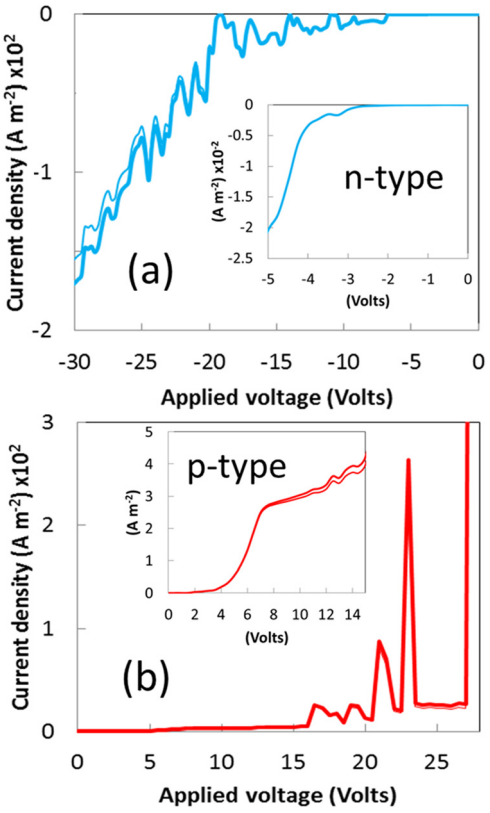

FIG. 4. Measured *I–V* characteristics for mercury-silicon Schottky diodes. (a) n-type silicon and (b) p-type silicon. The thin lines are the modified current densities obtained using Eqs. (2) and (3).

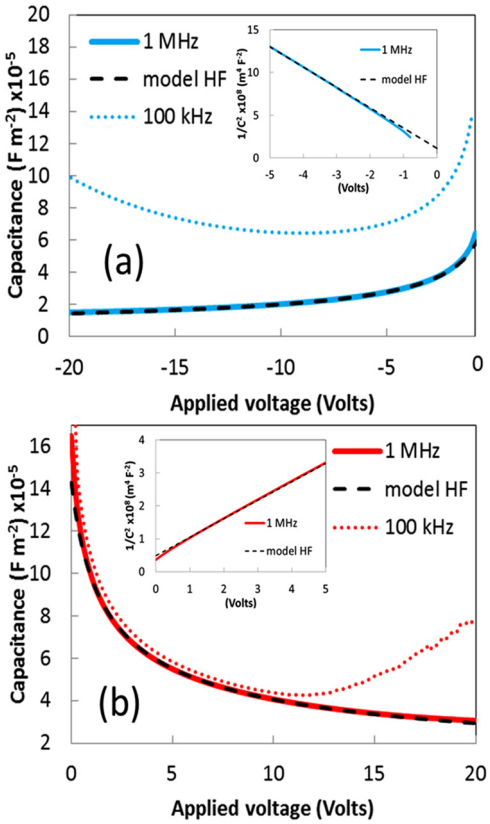

FIG. 5. Measured *C–V* curves for aluminum-silicon Schottky diodes formed using silicon wafers having the same doping density and surface treatment prior to Schottky formation as used for the electrowetting experiments. (a) n-type silicon and (b) p-type silicon. Measurement frequency = 100 kHz and 1 MHz. Insets show Mott-Schottky $1/C^2$ vs. V—plots at 1 MHz. The dashed curves are based on a depletion layer capacitance model [see Ref. 4].

Schottky formation (Hg and Al) was the same for the two experiments. An HF surface treatment of silicon prior to Schottky contact formation is known to result is a low surface state density[35] $D_s \sim 10^{10}$ states $m^{-2}\,eV^{-1}$.

The high frequency *C–V* measurements allow the extraction of the doping density of the wafers via a Mott-Schottky $1/C^2$ versus V plot shown in the insets to Fig. 5—at 1 MHz the measured capacitance is equal to the depletion layer capacitance as charge at the interface cannot follow the AC signal.[4] The doping levels of the n-type and p-type wafers were evaluated to be $5.22 \times 10^{14}\,cm^{-3}$ (8.66 Ω cm) (max: $5.47 \times 10^{14}\,cm^{-3}$, min: $5 \times 10^{14}\,cm^{-3}$) and $2.12 \times 10^{15}\,cm^{-3}$ (6.46 Ω cm) (max: $2.18 \times 10^{15}\,cm^{-3}$, min: $2.05 \times 10^{15}\,cm^{-3}$). The difference between the low frequency and high frequency *C–V* curves can be used to estimate[4] the surface state density D_s which we consider in a first approximation to be constant, although this is known not to be the case.[36] The *C–V* measurement yield values of D_s corresponding to 2.98×10^{11} states $m^{-2}\,eV^{-1}$ and 3.48×10^{11} states $m^{-2}\,eV^{-1}$ for the n-type and the p-type silicon surfaces used here. These measured values for the silicon surface state density D_s agree well with measured values for silicon surfaces[35] and also using Hg-Si system.[26–28] In addition, and as a comparison, *I–V* measurements were performed on the Al-Si Schottky diodes leading to the following results: $V_{bi} = 1$ V and 1.06 V - $\varphi_b = 0.78$ eV and 0.77 eV for n-type and p-type materials.

The *C–V* measurements also allow us to evaluate the series resistance R_s introduced by the finite conductivity of the silicon wafers. We measure $R_s = 850$ Ω (n-type) and 425 Ω (p-type) for Al-Si diodes having a surface area are comparable to the junction area of the Hg-Si diodes used for the electrowetting experiments.

As the capacitance of a Schottky diode is voltage-dependent we need to derive a modified Young-Lippmann equation to describe Schottky electrowetting. As a first approximation, by using a simple charge model of a Schottky junction[4]—taking into consideration surface states and the space-charge density in the semiconductor—one can obtain the following formula (see Ref. 30):

$$\cos\theta = \cos\theta_0 + \frac{2\sqrt{2q\varepsilon_r\varepsilon_0 N_D}}{3\gamma}(V_{bi} - V)^{\frac{3}{2}} - \frac{qD_s}{\gamma}(E_g - q\phi_0 - q\phi_{Bn})V, \quad (2)$$

where θ and θ_0 are described above, ε_r is the dielectric constant of the semiconductor, ε_0 is the permittivity of free space, q is the elementary charge, N_D is the doping density in the semiconductor (n-type), V is the applied voltage, V_{bi} is the built-in voltage of the diode,[4] and D_s is the surface state density,[4] γ is as above, E_g is the band-gap of the semiconductor, ϕ_0 is the energy level at the semiconductor surface,[4] ϕ_{bn} is the barrier height of the metal-semiconductor.[4] Note that, in contrast to EWOD, electrowetting-on-a-semiconductor depends strongly on the properties of the underlying semiconductor (doping type, N_D and ε_r) and the semiconductor

interface (D_s, V_{bi}, ϕ_0, and ϕ_{bn}). Equation (2) holds only in reverse bias; under forward bias, conduction occurs and the droplet will not spread out—as is seen in the measurements [Fig. 3].

We are in a position to plot the modified Young-Lippmann Eq. (2) in Fig. 3 by using the measured values of the doping densities N, the built-in voltages V_{bi}, the barrier heights ϕ_b and by using a surface tension of mercury equal to 486.5 mJ m^{-2} and an energy level at the silicon surface[4] φ_0 equal to 0.3 ± 0.36 eV. Using the extracted Schottky parameters it can be seen that Eq. (2) agrees very well with the contact angle measurements up to the point where contact angle saturation is observed due to conduction (as explained above).

In addition, the small signal areal capacitance values—obtained from the C–V measurements—can be used to calculate the stored charge Q at the Schottky junction at a given voltage—these values of Q can be then injected into a modified Young-Lippmann equation;[30] by doing this one obtains the short dashed lines indicated in Fig. 3. These data are seen to fit well with the contact angle variation obtained from the electrowetting measurements (open circles) using the capacitance measurements indicating that the electrowetting is determined by the space-charge and surface-charge of the Schottky diode. It is well documented that the capacitance of a Schottky diode is dependent on measurement frequency[37,38] and depends strongly on interface traps.[39,40] The observations here suggest that the areal capacitance associated with the electrowetting measurements is the capacitance associated with space-charge and surface states.

We now know that a voltage-induced modification of the contact angle—at constant droplet volume v_d—results in a modification of the surface area of the Hg-Si liquid-solid interface A_{ls}. As a consequence the current density $J_{meas} = IA_{ls}$—obtained from the I–V measurements - and the capacitance $C_{meas} = CA_{ls}$—obtained from the C–V measurements—are incorrect if we consider A_{ls} to be constant and should be modified using the following equation:

$$A_{ls}(\theta) = \left[\frac{2\sqrt{\pi}v_d \sin^3\theta}{(2+\cos\theta)(1-\cos\theta)^2}\right]^{\frac{2}{3}}. \quad (3)$$

This effect should be taken into consideration for electrical measurements using conducting liquid-semiconductor (e.g., Hg-Si)[26] and conducting liquid-insulator-semiconductor (e.g., Hg-SiO_2-Si)[26] systems if surface restriction techniques, such as an o-ring,[22,23] are not employed to fix the diode junction area. In order to obtain the true values of J (A m^{-2}) and C (F m^{-2}) from the measured I (A) and C (F), one should divide the measured values by the voltage-dependent contact area A_{ls}—obtained via electrowetting experiments—and not simply by the A_{ls} at *zero bias*. By using Eqs. (2) and (3) and the values of the contact angle saturation from the contact angle data, the real current densities at −30 V (n-type) and +40 V (p-type) [Fig. 4] are a factor of 0.9 and 0.84 smaller than J_{meas}—these are plotted as thin lines in Fig. 4.

Finally, it should be noted that, unlike the EWOD set-up, original wetting transitions can be observed using liquid-semiconductor (as reported here) and liquid-insulator-semiconductor junctions.[17] The use of semiconductor properties in wetting may have important applications, e.g., a combination of electrowetting and rectification could be useful in terms of energy harvesting[14] and microfluidic electronics.[41]

[1]F. Braun, Ann. Phys. Chem. **153**, 556–568 (1874).
[2]G. Lippmann, Ann. Chim. Phys. **5**, 494 (1875).
[3]R. T. Tung, Mater. Sci. Eng. R. **35**, 1 (2001).
[4]S. M. Sze, *Physics of Semiconductor Devices*, 3rd ed. (Wiley-Interscience, New Jersey, 2007).
[5]F. Mugele and J.-C. Baret, J. Phys. Condens. Matter **17**, R705 (2005).
[6]G. Beni and S. Hackwood, Appl. Phys. Lett. **38**, 207 (1981).
[7]M. G. Pollack, R. B. Fair, and A. D. Shenderov, Appl. Phys. Lett. **77**, 1725 (2000).
[8]H. J. Lee and C.-J. Kim, J. Microelectromech. Syst. **9**, 171 (2000).
[9]B. Berge and J. Peseux, Eur. Phys. J. E **3**, 159 (2000).
[10]T. Krupenkin, S. Yang, and P. Mach, Appl. Phys. Lett. **82**, 316 (2003).
[11]R. A. Hayes and B. J. Feenstra, Nature **425**, 383 (2003).
[12]H. You and A. J. Steckl, Appl. Phys. Lett. **97**, 023514 (2010).
[13]A. R. Wheeler, Science **322**, 539 (2008).
[14]T. Krupenkin and J. A. Taylor, Nat. Commun. **2**, 448 (2011).
[15]N. F. Mott, Proc. Cambridge Philos. Soc. **34**, 568 (1938).
[16]W. Schottky, Naturwiss. **26**, 843 (1938).
[17]S. Arscott, Sci. Rep. **1**, 184 (2011).
[18]P. Blood, Semicond. Sci. Technol. **1**, 7 (1986).
[19]D. Wei, P. Andrew, and T. Ryhanen, J. Chem. Technol. Biotechnol. **85**, 1547 (2010).
[20]P. Bergveld, Sens. Actuators B **88**, 1 (2003).
[21]M. J. Panzer and C. D. Frisbie, Adv. Mater. **20**, 3177 (2008).
[22]D. K. Donald, J. Appl. Phys. **34**, 1758 (1963).
[23]P. J. Severin and G. J. Poodt, J. Electrochem. Soc. **119**, 1384 (1972).
[24]M. Wittmer and J. L. Freeouf, Phys. Rev. Lett. **69**, 2701 (1992).
[25]Q. Wang, D. Liu, J. T. Virgo, J. Yeh, and R. J. Hillard, J. Vac. Sci. Technol. A **18**, 1308 (2000).
[26]H. J. Hovel, Solid-State Electron. **47**, 1311 (2003).
[27]Y-J. Liu and H-Z. Yu, J. Phys. Chem. B **107**, 7803 (2003).
[28]J. Y. Choi, S. Ahmed, T. Dimitrova, J. T. C. Chen, and D. K. Schroder, IEEE Trans. Electron Devices **51**, 1164 (2004).
[29]K.-S. Yun, I.-J. Cho, J.-U. Bu, C.-J. Kim and E. A. Yoon, J. Microelectromech. Syst. **11**, 454 (2002).
[30]See supplementary material at http://dx.doi.org/10.1063/1.4818715 for supplementary movies and supplementary information.
[31]A. F. Stalder, G. Kulik, D. Sage, L. Barbieri, and P. Hoffmann, Colloids Surf., A **286**, 92 (2006).
[32]F. Mugele, Soft Matter **5**, 3377 (2009).
[33]S. Chevalliot, S. Kuiper, and J. Heikenfeld, J. Adhes. Sci. Technol. **26**, 1909 (2012).
[34]H. C. Card, IEEE Trans. Electron Devices **23**, 538 (1976).
[35]H. Angermann, K. Kliefoth, and H. Flietner, Appl. Surf. Sci. **104/105**, 107 (1996).
[36]D. Vu, S. Arscott, E. Peytavit, R. Ramdani, E. Gil, Y. André, S. Bansropun, B. Gérard, A. C. H. Rowe, and D. Paget, Phys. Rev. B **82**, 115331 (2010).
[37]E. H. Nicollian and A. Goetzberger, Bell Syst. Tech. J. **46**, 1055 (1967).
[38]G. I. Roberts and C. R. Crowell, Solid-State Electron. **16**, 29 (1973).
[39]A. M. Cowley and S. M. Sze, J. Appl. Phys. **36**, 3212 (1965).
[40]J. Werner, K. Ploog, and H. J. Queisser, Phys. Rev. Lett. **57**, 1080 (1986).
[41]S. Cheng and Z. Wu, Lab Chip **12**, 2782 (2012).